

New concepts for nanophotonics and nano-electronics

## Challenges and potential of new approaches for reliability assessment of nanotechnologies

Laurent Béchou<sup>a,\*</sup>, Yves Danto<sup>a</sup>, Jean-Yves Deletage<sup>a</sup>, Frédéric Verdier<sup>a</sup>,  
Yannick Deshayes<sup>a</sup>, Sébastien Fregonèse<sup>a</sup>, Cristell Maneux<sup>a</sup>, Thomas Zimmer<sup>a</sup>,  
Dominique Laffitte<sup>b</sup>

<sup>a</sup> Laboratoire IMS, UMR CNRS n° 5218, 351, Cours de la Libération, 33405 Talence cedex, France

<sup>b</sup> 3SPhotonics, Route de Villejust, 91625 Nozay cedex, France

Available online 15 February 2008

### Abstract

Reliability assessment of components, integrated circuits or micro-assembled devices, is undoubtedly identified as one of the major factors conditioning the on-going development of microelectronics. In the same way, growing market penetration by nanotechnologies is clearly related to the imperative demonstration of satisfactory built-in operational reliability with respect to actual severe standards. This situation requires a specific effort on built-in reliability. These considerations must be integrated, as early as possible at the beginning of the development ‘top-down’ and the ‘bottom-up’ approaches. Reliability issues cover extremely large scientific fields such as physics, material science, electrical transport, thermal phenomena, coupling interfaces between optics and electronics, statistical models, etc.

The objective of this paper deals with the presentation of new, original methodologies for reliability assessment, coming from studies in the IMS Laboratory, in close collaboration with industrial and academic partners. These new approaches are based on the combination of the physical laws of failure, behavioral simulations and statistical methods, adding inevitable parametric dispersions to extrapolate failure rates and lifetime in operating conditions. Some results are presented and analyzed on micro-assembled technologies and photonic components for high-rate optical links. The main goal is to discuss their potentiality and applicability field with a view to intrinsic nanodevices reliability assessment in operating conditions. *To cite this article: L. Béchou et al., C. R. Physique 9 (2008).*

© 2007 Académie des sciences. Published by Elsevier Masson SAS. All rights reserved.

### Résumé

**Challenges et potentialités de nouvelles approches pour l'évaluation de la fiabilité des nanotechnologies.** L'évaluation de la fiabilité des composants, circuits intégrés ou composants microassemblés, est incontestablement identifiée comme un des facteurs majeurs conditionnant la poursuite du développement de la microélectronique. De la même façon, la pénétration croissante des marchés, par les nanotechnologies, sera liée à la démonstration urgente d'une fiabilité opérationnelle construite en relation avec les standards actuels très exigeants. Cette situation nécessite un effort spécifique sur les méthodes de construction et de démonstration de la fiabilité. Ces réflexions doivent être intégrées, dès les phases de conception, en considérant deux approches clés liées aux modes de fabrication des dispositifs nanotechnologiques : les approches ‘top-down’ et ‘bottom-up’. La problématique de la fiabilité est, par définition, extrêmement large et couvre à la fois les questions relatives à la physique et à la physico-chimie des matériaux, aux phénomènes de transport électrique, aux phénomènes thermomécaniques, interfaces de couplage optique/électronique, aux modèles statistiques, etc.

\* Corresponding author.

E-mail address: [laurent.bechou@ims-bordeaux.fr](mailto:laurent.bechou@ims-bordeaux.fr) (L. Béchou).

L'objectif de cette contribution est de présenter les résultats de nouvelles méthodologies d'évaluation de la fiabilité, issues des travaux du Laboratoire IMS en étroite collaboration avec des partenaires industriels et universitaires. Ces approches spécifiques sont basées sur l'utilisation combinée de lois physiques de défaillance, de simulations comportementales et de méthodes statistiques intégrant une variabilité technologique inévitable pour extrapoler des taux de défaillance et des durées de vie en conditions opérationnelles. Des exemples d'application sont présentés et analysés sur des technologies microassemblées et composants optoélectroniques pour liaisons optiques à haut débit. Le but principal est de discuter de leurs potentialités et de leur champ d'application en vue de l'évaluation de la fiabilité intrinsèque de dispositifs nanotechnologiques en conditions opérationnelles. **Pour citer cet article : L. Béchou et al., C. R. Physique 9 (2008).**

© 2007 Académie des sciences. Published by Elsevier Masson SAS. All rights reserved.

*Keywords:* Reliability; Failure mechanisms; Lifetime; Behavioral modeling; Nanotechnologies

*Mots-clés :* Fiabilité; Mécanismes de défaillance; Durée de vie; Simulations comportementales; Nanotechnologies

## 1. Introduction

Micro-assembled technologies and microsystems and, soon, nanodevices, are intended to be systematically combined and integrated in electronic functionalities. These technologies evolve very rapidly towards submicronic and nanometric scales, associated to a higher and higher complexity, increasing their susceptibility to stress environments and the difficulty to both assess robustness and predict lifetime in operating conditions. Very high levels of reliability are required in most of industrial applications, such as the automotive, and more generally, transportation industry, mobile communications or medical instrumentation. For example, the automotive industry is now focused on failure rates lower than 10 FITs (1 FIT is the usual unit corresponding to a proven failure over  $10^9$  hours). In many other applications (space, defence, sub-marine telecommunications), it is practically a level of 'zero' defect, which is mandatory over a given lifetime depending on the mission profile. In the case of electronic devices or sub-systems, there is a requirement to guarantee an upper limit of failure rate, generally corresponding to the maximum expected lifetime of the system in which the device is incorporated.

The first key element, which must be taken into account for the development of micro and nanotechnologies, deals with the fact that these devices will be rapidly used in conjunction with more mature technologies in a market whose requirements for reliability prediction still remain based on harsh actual standards. Thus, there is very little margin between the technological development phase and the high reliability demonstration of a nanotechnological device, because of the risk of this remaining a technological 'curiosity' for a long time. Consequently, assessment of micro and nanocomponents reliability is essential to validate their performance and enlarge their dissemination [1]. It must be taken into account, from an upstream point-of-view, during the choice and the development of new processes (reproducibility and repeatability), but also from downstream, in an industrial phase of component qualification. So this condition requires a complete renewal of methodologies for reliability demonstration. In this context, the basis of high reliability must integrate into the level of design, technological choices, process control and physical modeling of failure mechanisms, one of the objectives being to guarantee failure distributions as tight as possible at the end of device lifetime. The foundation of an 'active' approach of reliability demonstration involves a thorough analysis and modeling of the physical degradation mechanisms of the components under operation to internal stresses (technologies), and/or external stresses (environmental). Several steps must 'operational' reliability, i.e. through the specified conditions of industrial production (variability of technological parameters) and use (variability of the mission profiles). It can be easily understood that the way can be long, in particular for emergent nanotechnology devices whose manufacturing processes and the functional limits are far both from being determined and stabilized. The following phases can resume the next decisive technological requirements for reliability assessment of nanotechnologies:

- A precise description of the mission profile in order to derive a good representation of the stress field acting on the ageing component; this point is essential, especially to design an accelerated testing program in view to assessing critical points;
- The modeling of degradations, with the determination of early degradation indicators and failure mechanism analysis. This crucial phase belongs to the development of new technologies and can generate important feedback on the design;

- The introduction of both material and process variations in order to evaluate their impact on product lifetime distribution. This last point has to be combined with mission profile distribution.

## 2. Classification of nanotechnologies

The principle of early, built-in ‘upstream’ reliability in the design phases and manufacture processes being considered as essential, it still remains that, to clarify the problematic of nanotechnologies, two main types of classification must be distinguished.

### 2.1. ‘Top-down’ approach

In the field of nanoelectronics resulting from microelectronic technologies, this approach corresponds to an extension of the processes towards nanometric dimensions (‘ultimate’ technology MOS, spintronics, nanophotonics ...). These technologies strongly see an increase in their criticality, i.e. their sensitivity with respect to weak variations of technological parameters, and facing technological fluctuations directly resulting from dimension shrinkage of the elementary components towards the molecular or atomic scales. For instance, ‘ultimate’ MOS technologies are confronted with electrostatics of random discrete dopants, line-edge roughness of the gate edge (LER) influencing the effective length of the channel, ... etc. inducing much dispersion of the main electrical parameters, such as the electrical threshold voltage of transistors as shown in Fig. 1. The standard deviation in threshold voltage is thus strongly dependent on the magnitude of the fluctuations which increases dramatically as the channel length reduces from 300 nm to 100 nm. In the case of sub-100 nm devices, these effects become more and more crucial. For example, A.R. Brown reports that the standard deviation in threshold voltage can reach 0.07 V for a 4 nm device. Assuming a  $\pm 3\sigma$  spread around the mean in a normal distribution of  $V_T$ , this gives a range of approximately  $\pm 0.2$  V around the nominal threshold voltage of  $V_T \approx 0.2$  V. This means that a significant fraction of the devices on a chip with a billion transistors will not turn OFF. The dependence of  $\sigma V_T$  on channel length and width is stronger than the well-known  $1/(W \times L)^{1/2}$  relationship expected for threshold voltage fluctuations induced by random dopants in the channel region [2].

Amplification of degradation mechanisms by ageing must be added to these previous effects, such as degradation of gate oxides by ‘hot’ carrier injection, strongly affecting lifetime [3]. The introduction of new steps in photolithographic processes and new materials (insulating of the grid, interconnections), requires a phase of accurate reliability assessment. However, this must be carried out based on prior scientific and technical knowledge and lead quickly to results, because of the actual requirements of reliability for an integration of these devices in the industrial, technological environment. Among these failure mechanisms, we can list [4–6]:

- ‘High K’ gate dielectric: breakdown phenomenon, charges trapping, stability of charges, ... ;
- Copper/dielectric ‘low K’ interconnections: electromigration, stress voiding, thermomechanical effects, mechanical resistance, dielectric impact (porosity, thermal conductivity);

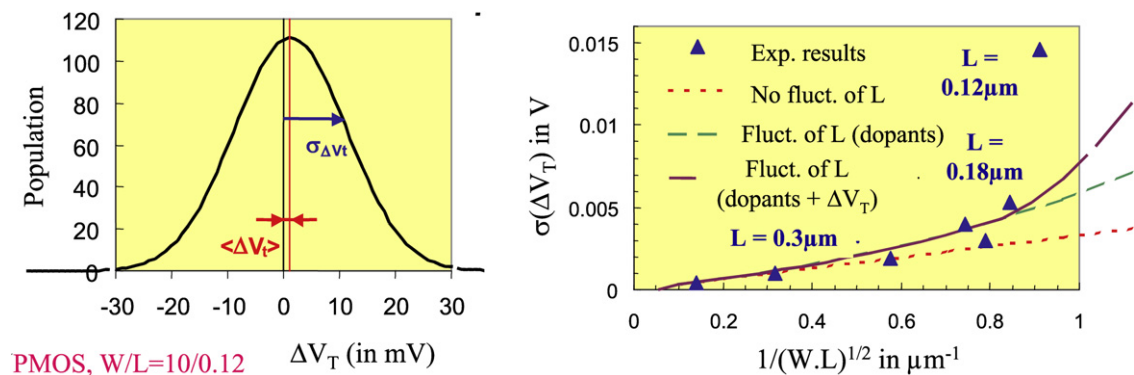


Fig. 1. The effect of technological fluctuations on the threshold voltage of deep-submicron MOS transistors.

Fig. 1. Effets de fluctuations technologiques sur la dispersion des tensions de seuil de transistors MOS largement submicroniques [7].

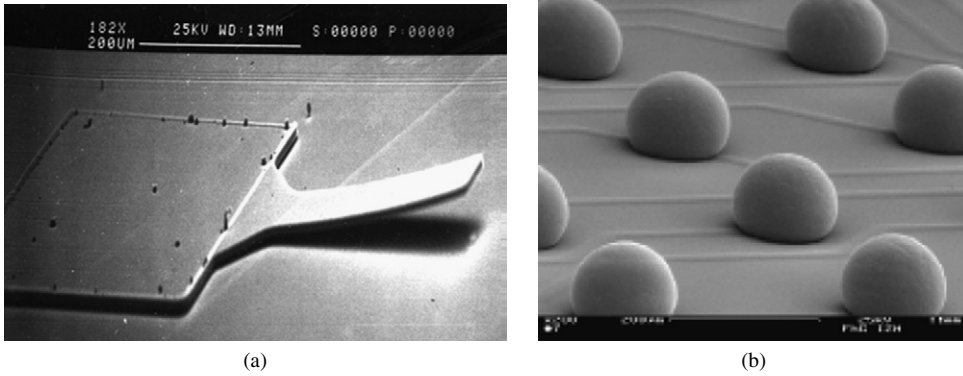


Fig. 2. (a) SEM photograph of polysilicon cantilever, (b) SEM photograph of Flip-Chip micro-assembly.  
 Fig. 2. (a) Image MEB d'un cantilever en polysilicium, (b) Image MEB d'un microassemblage de type Flip-Chip [8].

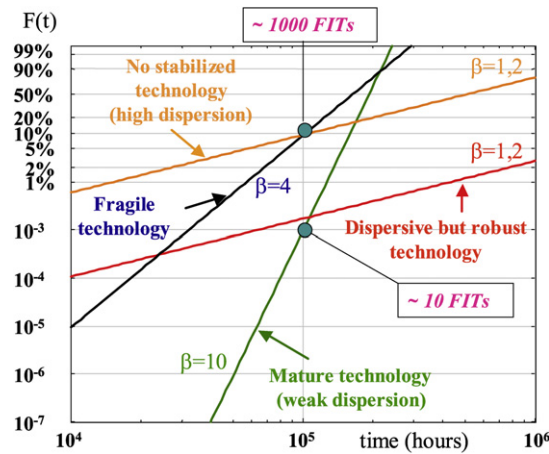


Fig. 3. Impact of technological maturity on potential reliability.  
 Fig. 3. Impact de la maturité d'une technologie sur la fiabilité potentielle.

- Metallic gates: diffusion of grid into insulator, susceptibility to oxidation, thermal coefficient expansion (TCE) mismatch, impact of highly focused ion beam implantation, . . .

The expression ‘micro-nano’ does not only address the phenomenon of dimensional scale decrease from a uniform way. It also includes the ‘micro-object’ environment constituted by microsystems. In this case, the dimensional factor is not essential, but all the multi-material and multi-process aspects are also predominant. From a reliability point of view, questions related to the response of heterogeneous materials to common stresses, as well as three-dimensional configurations do not allow one to limit the study to a monodimensional mode. In this category, we not only find microsystems but also microassemblies and micropackaging (Fig. 2). It should be remembered that these earlier technologies must follow the integration progresses of the semiconductors, similar, in dimensional terms (‘Ball Grid Array-BGA’, ‘Flip-Chip’, ‘Chip Scale Package-CSP’, . . .) and in terms of complexity (3D packages, Plastic On Package, Lab On Chip . . .). Thermal and mechanical phenomena, corrosion, intermetallic growth, interface pollution, electromigration, moisture propagation in encapsulation materials, . . . are particularly crucial but representative of the complexity of microsystems, but also at the short-term for nanosystems. In general, weak maturity involves huge parameter dispersion on component population. Such dispersion involves a greater spreading of failures and so onto the lifetimes of a component batch during a qualification process (Fig. 3). In a ‘Weibull-like’ representation, regularly applied in such experimental procedure, (see Eq. (1)), these results mostly generate a weaker slope ( $\beta$ ).

$$F(t) = 1 - e^{-(t/\alpha)^\beta} \tag{1}$$

with  $(\alpha, \beta)$ : parameters of Weibull law.

For nano-architectures, circuit reliability reflects its ability to sustain correct operation considering the occurrence of runtime failure(s) or interference(s), traditionally referred as faults. Three types of fault can be considered [9–11]:

- Permanent faults, due to irreversible changes in circuit structure; these kinds of fault are reduced by an appropriate design and manufacturing methods. In current processes, permanent faults can be considered negligible;
- Intermittent faults are caused by variations in the manufactured structure that were not detected as defects, and that appear under specific conditions depending on supply voltage, temperature, etc. Since these are related to parametric variations, this type of fault tends to increase with technology scaling;
- Transient faults, or soft errors, caused by alpha or neutron particles, electrostatic discharge, thermal noise, cross-talk, etc. The most common physical mechanisms are related to alpha particles and cosmic radiation, which are related to materials and processes. High-energy cosmic neutrons are found to be the predominant sources of soft errors in more advanced manufacturing processes. The reduction in voltage levels and the increase in device operation frequency greatly enhance the susceptibility of the circuits to soft errors. For this reason, transient faults are the more critical source of faults in nano-architectures.

One metric that represents the soft-error rate (SER) is also the failure in time (FIT). In advanced computer systems, the fault rate for most fault sources is less than 150 FITs, while for SER, the value can be 50 000 FITs or more. This SER level represents almost a soft error every two years. Soft errors are an increasing threat to either logic circuits or interconnections in nanotechnologies. The effect of a soft error in sequential logic is known as a single-event upset (SEU), where the state of a memory cell, flip-flop or latch is reversed. For combinational logic, the effect is known as a single-event transient (SET) and is characterized by a voltage pulse. Formerly negligible, SETs soft errors are becoming important as circuits scale down and operating frequencies increase, due to a higher probability of a SET propagation to multiple paths in the circuit and capture of the voltage pulse by storage cells (latches and flip-flops). According to predictions, SETs will achieve the same probability of SEUs for 65 nm technologies.

Cross-talk is also becoming a critical issue in the design of nanometric circuits, especially because of interconnection wires. In order to avoid a considerable increase in wire resistance, wire height is not scaled down at the same rate as its width, leading to an increase in the coupling capacitance between adjacent wires. However, the most threatening source of transient faults in future circuits will be thermal noise. The problem is related to thermal energy in the circuits, that induces false bit-flips in devices. Despite the fact that the ITRS shows CMOS evolution until the 14 nm node, in 2020, scaling is strongly menaced by thermal noise and some studies predict the end of traditional scaling around the years 2008–2010 with nodes of 30–40 nm. Supply voltage reduction can help control thermal dissipation despite the present CMOS circuit architecture which tends to enhance SER. Considering the reliability scenario, as operating frequencies and device densities increase, fault-tolerant design techniques gain importance to reduce SER in integrated circuits. Traditionally applied in the design of memories, fault-tolerant methods will be also required for logic in nanometric designs. Besides the application of the usual fault-tolerant methods, that are able to recover a single fault, new ones must be researched, since multiple simultaneous transient faults are predicted for future technologies.

## 2.2. 'Bottom-up' approach

In the case of nanotechnologies directly resulting from material science (chemical synthesis) and the utilization of their specific properties (at the molecular or atomic level), reliability must imperatively be approached at the preliminary phases of development. Each new material, such as carbon nanotubes, fluorescent nanocrystals, organic electronics . . . , requires also new processes which are not yet stabilized. Potential reliability must be integrated through a choice of process, tolerant to defects, constituting one of the first actions to be carried out in a phase of research and development. Knowing that these processes are controlled on collective or macroscopic modes (and not at the level of the elementary components), technological choices must be considered from a reliability point of view, i.e. by taking into account 'materials' aspects in relation to chemical stability, self-recovery of defects, insensitivity to non-functional elements, and self-organization. The objective is to compensate some high-dispersion spread of active elements and the intrinsic weakness of manufacturing yields, i.e. on the level of the individual component. Due to their mechanical and electronic properties for potential applications in nano-electronic devices and nano-electromechanical

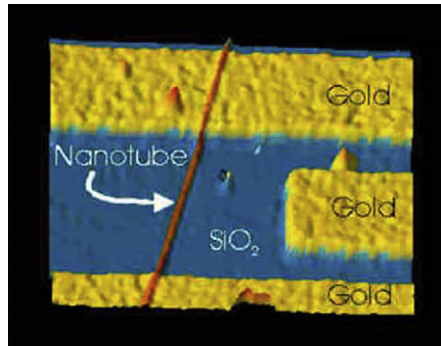


Fig. 4. Example of CNT-based transistor illustrating the ‘bottom-up’ approach.

Fig. 4. Exemple de transistor à CNT illustrant l’approche ‘bottom-up’ (source IBM).

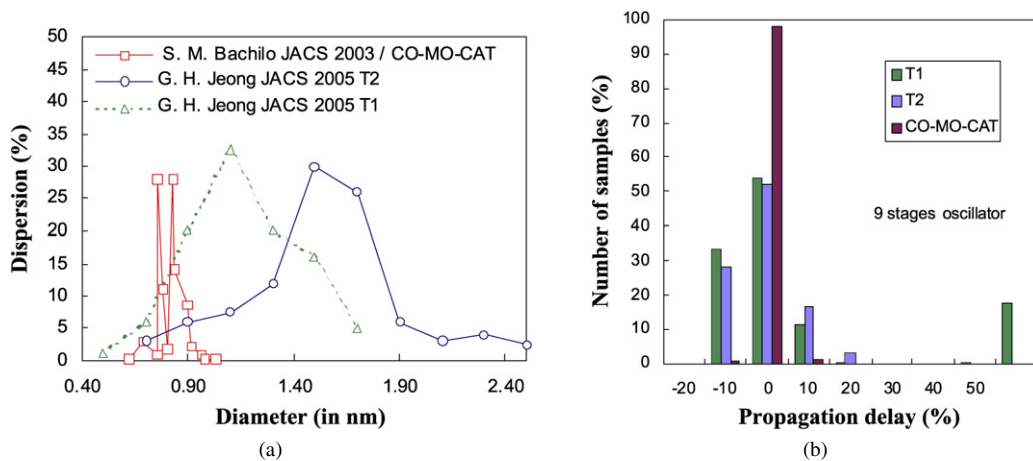


Fig. 5. Technological fluctuation effects on propagation delay of CNTFET-based 9 stages oscillator: (a) Example of dispersion of nanotubes diameter; (b) Dispersion impact on electrical performances.

Fig. 5. Effets de fluctuations technologiques sur le retard de propagation d’un oscillateur à 9 étages à base de CNTFET [18,19] : (a) Exemple de dispersion du diamètre des nanotubes ; (b) Impact de la dispersion sur les performances électriques.

systems (NEMs), Carbon NanoTubes (CNTs) are the object of intensive research interests. Fig. 4 shows an experimental device of a CNT-based transistor developed by IBM, and Fig. 5 reveals the strong influence of technological fluctuations effects on the propagation delay of CNTFET-based oscillator. Challenges must then be focused on the following aspects:

- Carry out ‘macroscopic’ control or ‘collective’ of the processes in spite of an ‘intrinsic’ disorder;
- Strive quickly towards the notion of a manufacturing yield;
- Use the potential of self-organization of microscopic structures;
- Recovery or neutralization of the non-functional components;
- Interface of connection with the micrometric environment or the entire system.

### 3. Specific challenges of nanotechnologies

The ageing of components results from a set of physico-chemical processes that appears by drifts of characteristics (functional or not). These expected degradations are specific to the component, but also strongly depend on its utilization and the environment, in their nature and their kinetics. Long-term, this damage, progressive or more rapid, led to a decrease in the system functionality (associated with criterion definition) and thus to failure. Whereas for ‘top-down’ nanodevices, we have the knowledge of the principal mechanisms of degradation resulting from micro-electronics, for

new technologies based on a ‘bottom-up’ approach where the introduction of new materials, new processes and the exploitation of properties, up to now not really exploited, will inexorably initiate new behavior.

First of all, positive factors go in the direction of an increased intrinsic robustness of nanotechnologies. These devices are little sensitive to mechanical shocks, and more generally reveal a good mechanical and thermomechanical resistance, because of their extremely favorable dimensions. Internal thermal stresses will be weak due to the low electrical dissipation characterizing the majority of these devices [12]. However, there are also factors which reinforce the intrinsic criticality: the size of the active elementary structures becomes similar to that of defects. For example, in the case of single wall CNTs with small diameters ( $< 0.5$  nm), experimental and theoretical efforts have actually been devoted to atomistic failure mechanisms depicting strains and fracture, in particular due to the bending process [13].

Because of importance of surfaces, the sensitivity to aggression can increase overall. For example, in the case of actual laser diodes, the quality of the interfaces represents a critical issue for reliability. Heterostructures are inherently unstable with respect to atomic interdiffusion across interfaces. This instability is enhanced by stresses and is an important source of point defects. These point defects act as non-radiative recombination centers assisting the formation of new point defects by the RERD mechanism. This feedback mechanism leads to migration and condensation of point defects, forming precipitates or small dislocation loops affecting quantum efficiency and reducing the lifetime of such a device [14]. The impact of the preparation quality of active buried optical waveguides (ridge) or passive waveguide (tapers) and the steps of epitaxy overgrowth after RIE etching of the active zone can also locally generate zones of strong stresses and migrations of dislocations towards the active zone under temperature increase [15]. So nanophotonics based on waveguides using heterostructures (InGaAsP/InP, ...) or a photonic crystal nanocavity with a quality of interfaces free from defects for a most favorable optical confinement must be required to guarantee long lifetime for new photonic architectures [16].

One can also predict a susceptibility to electric overstress, of the electrostatic discharge type (ESD), because the internal electric signals are weak. The increasingly recurrent presence of organic materials, in the manufacturing processes (passivation, active zone, confinement, ...), will probably reinforce the question of their chemical stability and its impact on reliability at long-term. Lastly, it is necessary to consider the question of connectivity towards the macroscopic environment with the vast dimensional gap [17].

#### 4. New approaches for reliability assessment of nanotechnologies

The objective of this section is to present the results of new approaches, resulting from studies of the IMS laboratory in close cooperation with industrial partners and academic laboratories. These specific approaches are based on the mutual use of both physical degradation laws deduced from accelerated ageing tests, behavioral modeling and statistical methods taking into account technological variability (related to inevitable process dispersion data), but also the low number of tested samples due to the lack of maturity. In order to satisfy the demanding requirements encountered in nanotechnologies, especially to increase manufacturing yield and to reduce time-to-market, there will be a strong motivation to focus more on extrapolated cumulated failure rates and lifetime distributions allowing us to calculate first times to failure, rather than a classical prediction using MTTF or median life, in operational conditions of actual microelectronic components with at short-term, an objective of reliability “simulation” [20]. The aim is to analyze their potentialities and the prospects for applicability, regarding the actual technological limitations of nanotechnologies.

##### 4.1. Contribution of mixed models – impact of technological process dispersion [21,22]

The first case deals with some results trying to derive reliability behavior of highly integrated microassemblies (BGA, CSP), submitted to a thermal cycle mission profile, as is now common in many applications. In the field of surface mounted technology (SMT), reliability testing becomes longer and increasingly expensive. This is due to the large variety of technological features that can be encountered even on the same board where different package sizes and types can coexist. In this case, it is important to identify the most critical attribute and to try to simplify the reliability test procedure through the definition of a ‘generic’ accelerated test, performed on only one assembly and extensible to package configurations. Soldering between package and board is particularly affected by thermal cycling, so that solder joints in leaded and unleaded packages are in most cases a critical part of the assembly, and this has a major influence on reliability. Failure cracks appearing after a number of thermal cycles depend on many

Table 1  
Summary of some cycle (time) to failure laws

Tableau 1  
Résumé des lois donnant le nombre de cycles à la défaillance

Law	Equation
Coffin–Manson	$N_f = (\Delta\gamma/\varepsilon_0)^{1/c}$ $c, \varepsilon_0$ : coefficients related to the technology
Engelmaier	$N_f = \frac{1}{2}(\Delta\gamma/2\varepsilon_0)^{\frac{1}{-0.442-0.0006T_{sj}+0.0174\ln(1+f)}}$ $T_{sj}$ : mean solder joint temperature during one cycle $f$ : number of cycles per day
Norris–Landzberg	$N_f = C f^m \Delta\gamma^{-n} e^{\frac{E}{kT}}$ $f$ : number of cycles per day $m, n$ : coefficients related to the technology

factors, mainly on TCE mismatches between substrate, lead and package, on package size, and on lead stiffness. In BGA technology, the poor compliance of the balls makes assembly critical to thermal cycling since a large size and TCE mismatches are combined. The number of cycles to failure of a given assembly submitted to thermal cycling is basically described by the well-known Coffin–Manson equation, as reported in Table 1. In this equation,  $\Delta\gamma$  is the strain rate in the solder joint. Engelmaier has reported coefficients  $c$  and  $\varepsilon_0$  to the technology characteristics and temperature conditions. A more explicit relationship to temperature cycle frequency has been proposed by Norris–Landzberg.

However, the evolution from degradation to crack induced failures can be followed by the microstructure progression under cycle stress. In the case of  $\text{Sn}_{63}\text{Pb}_{37}$  solder joints, a more accurate degradation evolution can be obtained by analyzing the lead rich phase coarsening. Using a fixed procedure, the mean lead phase coarsening  $\Delta S$  can be observed in a solder joint cross-section using SEM up to the apparition of cracks in the most strained region (corner). In previous studies, such an analysis has conducted to the fitted equation (2):

$$\Delta S = A \Delta\gamma^b \sqrt{N_c t_p} \exp\left(-\frac{E_a}{kT}\right) \quad (2)$$

where  $A$  is a constant,  $E_a$  the activation energy (0.45 eV in our experiment),  $N_c$  the cycle number and  $t_p$  the dwell time at the upper temperature  $T$ .

It is emphasized that  $\Delta\gamma$  is in this case the maximum strain rate, necessarily determined in the most strained region where the crack is expected to be initiated. A crack appears when a limit value of  $\Delta S$  is reached. The exponent  $b$  is technology dependent and must be experimentally derived. In this study, a value  $b = 0.5$  suits experimental results. It must be noted that the determination of local maximum strain  $\Delta\gamma$  can exclusively be done by Finite Element Modeling (FEM) simulation of the assembly. Experimental degradation curves using lead phase coarsening are well fitted when maximum total shear strain is extracted from one complete simulated cycle (not considering the first one). The location of the maximum cumulated plastic strain in the balls determined simulations and the position of the observed crack initiation and propagation are well matched in the upper region of the ball (as shown on Figs. 6 and 7).

This region corresponds also to the most perturbed microstructure area as shown by SEM analysis (Fig. 7). The number of thermal cycles of the accelerated ageing test can be adjusted to wait either for the complete off-state of the solder connection or crack initiation. In this last case, a direct analysis of the solder joint has to be made at least on the most stress exposed bumps. This procedure increases the experimental observation since cross-section and direct observations are performed, but it leads to a significant shortening of the test. To go further in the time reduction, phase coarsening evolution ought to be considered as a reliability indicator, through an extrapolation of the degradation law. However, such a procedure should be available only if a stable soldering process can be guaranteed. In this case, the number of cycles to failure ( $N_{c2}$ ) in given operational conditions ( $T_2, t_{p2}, \Delta\gamma_2$ ) will be obtained from the results of accelerated test ( $N_{c1}, T_1, t_{p1}, \Delta\gamma_1$ ) using Eq. (3) deduced from Eq. (2). Experiments were made with two different configurations: (CSP48) and a PBGA, both on the same board. We will consider operational conditions as:  $0^\circ\text{C}/+80^\circ\text{C}$  representing automotive dash-board conditions and  $t_{p1}/t_{p2} = 10.33$  fully functional boards coming from a mobile phone assembly line were used for the study. Three-Dimensional Finite Element analysis was performed



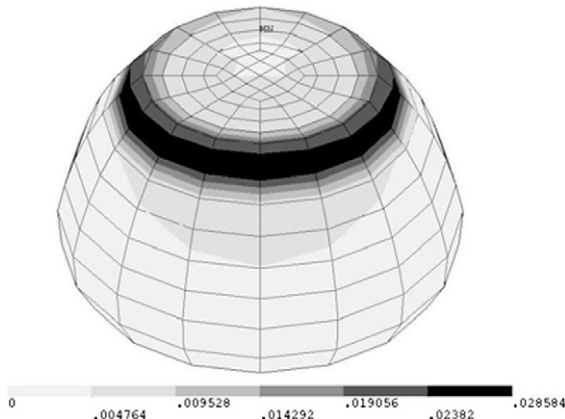


Fig. 6. Maximum cumulated plastic strain mapping of the most critical ball of a CSP48 assembly.

Fig. 6. Cartographie du maximum de déformations plastiques accumulées de la bille la plus critique d'un assemblage CSP48.

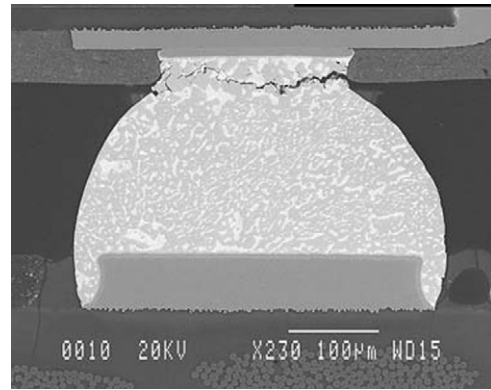


Fig. 7. SEM view of a complete crack at the solder joint/pad interface of a CSP48 assembly after 1200 cycles  $-55\text{ }^{\circ}\text{C}/+125\text{ }^{\circ}\text{C}$ .

Fig. 7. Vue au MEB de la fissuration complète à l'interface joint de brasure/plage de report d'un assemblage CSP48 après 1200 cycles  $-55\text{ }^{\circ}\text{C}/+125\text{ }^{\circ}\text{C}$ .

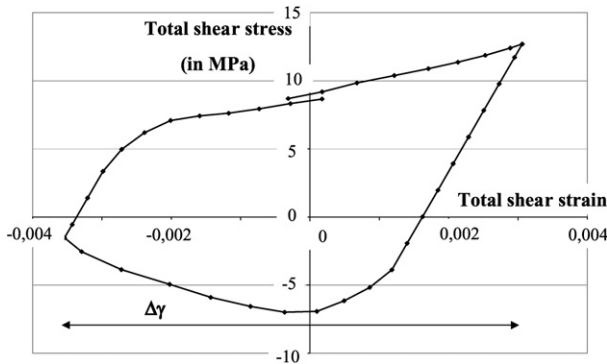


Fig. 8. Total shear stress strain curve after one thermal cycle.

Fig. 8. Courbe totale contrainte-déformation après un cycle thermique.

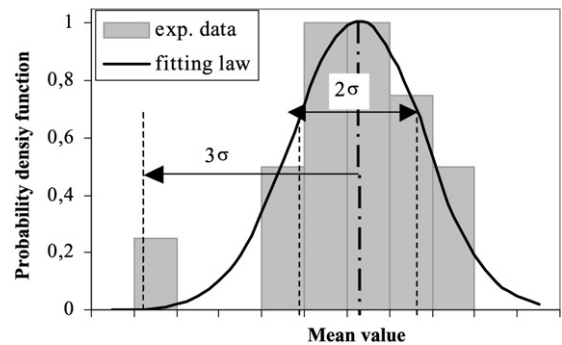


Fig. 9. Normalized probability density function (pdf) of solder joints height from manufacturing process data.

Fig. 9. Fonction de densité de probabilité de la hauteur des joints de brasure issue des données de processus de fabrication.

using ANSYS software to evaluate  $\Delta\gamma$  strongly dependent of many variables like material properties, geometric dimensions and manufacturing processes deviations which must be considered as random variables to evaluate solder joint fatigue life distributions [23]. Static and isothermal thermomechanical analysis was performed to evaluate  $\Delta\gamma$  taking into account stresses and strains due to TCE mismatch among materials (Fig. 8). Geometrical input data for FEM simulations are issued from process control. Variations of one geometric dimension have been taken into account: the variability of solder joints height (Fig. 9).

Due to the long computation time (about 24 h per test), only 4 values of are simulated for each configuration and each thermal cycle conditions (accelerated and operational conditions). The number of cycles to failure is assumed to be expressed by Eq. (4). Numerical computations are performed to obtain the whole distribution of the failure dates, due to the dispersion of  $\Delta\gamma$ . The scale factor ( $N_0$ ) is adjusted on the base of the ageing results in order to obtain the equivalence between experimental mean life and the predicted value (see Table 2). With Eq. (3), the acceleration factor, user conditions and the corresponding  $\Delta\gamma$  distribution are input to calculate an extrapolated distribution of failures, as represented by Fig. 10.

By self-consistence with experimental fits, the simulated data are roughly approximated by the 2 parameters of the Weibull law. Another important result from the previous data is that the effective acceleration factor, which is not constant along the whole device lifetime.

Table 2

Number of cycles to failure for CSP and BGA micro-assemblies, after accelerated stress compared to operating conditions

Tableau 2

Nombre de cycles à la défaillance après le test accéléré comparé aux conditions opérationnelles

		Experiments		Computed	
		mean	$\sigma$	mean	$\sigma$
–55 °C/+125 °C (accelerated test)	CSP48	1183	269	1275	435
	PBGA192	1777	215	1900	602
0 °C/+80 °C (operating conditions)	CSP48	–	–	13 800	4500
	PBGA192	–	–	52 000	13 000

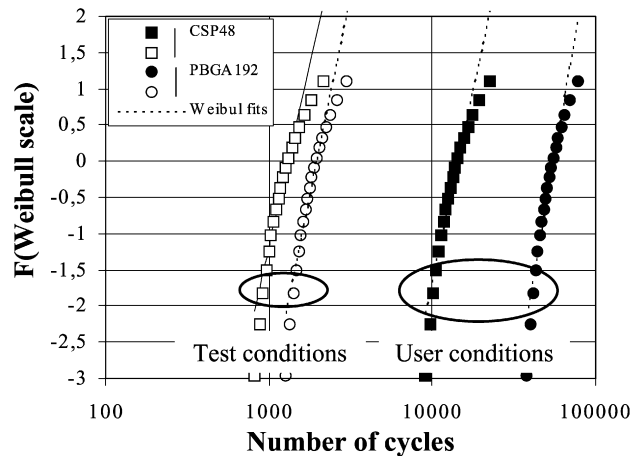


Fig. 10. Weibull plots for reliability of micro-assemblies in the accelerated test and the predicted ones for operating conditions.

Fig. 10. Graphes de Weibull des microassemblages en tests accélérés et extrapolés pour les conditions opérationnelles.

$$AF = \frac{N_{c2}}{N_{c1}} = \left( \frac{\Delta\gamma_1}{\Delta\gamma_2} \right)^{2b} \frac{t_{p1}}{t_{p2}} \exp \left[ \frac{2E_a}{k} \left( \frac{1}{T_2} - \frac{1}{T_1} \right) \right] \quad (3)$$

$$N_{cf} = N_0 \Delta\gamma^{-2b} \exp \left( \frac{2E_a}{kT} \right) \quad (4)$$

#### 4.2. Statistical approach for reliability prediction of photonic components [24–26]

Recent developments in photonic telecommunications still imply very high performance of transmitters (single mode Laser diode), receivers (APD photodiode) and in-line optical amplifiers (EDFA or SOA). These transmissions and their reliability requirements are generally divided into two main fields:

- Terrestrial applications (100 to 1000 km) with failure rate below 500 FITs over 15 years;
- Sub-marine applications (1000 to 10 000 km) below 100 FITs over 25 years.

The traditional approach for reliability demonstration of photonic components is drawn from international standards representing a useful guideline. From these tests, a lifetime distribution can be extracted and weighted by an upper confidence level (UCL). However, regarding actual levels of reliability related to long times to failure and very low failure rates, it is more and more common, that failure criterion cannot be reached until the end of the test and the determination of lifetime distribution increases dramatically. Due to failure processes (intrinsic failures with latent defects) being eliminated, for the most part by burn-in tests, and also wear-out failures (extrinsic failures) being rejected to very long time of life, the essential zone for reliability evaluation is the operating life as illustrated by the well-known ‘Roller-coaster’ curve. The problem is that, in this zone, the failure rate is so low that it will be very com-

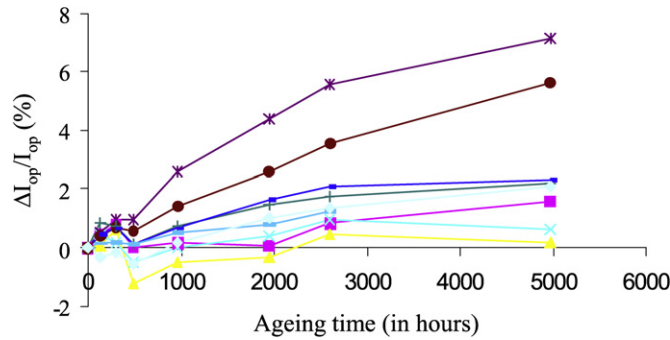


Fig. 11. Experimental drifts of bias current ( $I_{op}$ ) versus ageing time of 1.55  $\mu\text{m}$  DFB laser diodes.

Fig. 11. Variations expérimentales du courant d'alimentation ( $I_{op}$ ) en fonction du temps de vieillissement de diodes laser DFB 1,55  $\mu\text{m}$ .

plex to evaluate. Moreover, in particular for photonic technologies, the population tested is traditionally composed of a low number of samples. In this case, two solutions are suitable to reach the failure criterion set and to predict the lifetime:

- Strongly increase the acceleration factor using higher test temperatures or test current densities;
- Greatly increase duration of tests.

Nevertheless, these conditions are high-cost, time consuming and cannot give a complete distribution of times to failure with a negative impact on market penetration and profitability. For example, these ageing tests must be performed on more than 100 components aged during 10 000 hours mixing different temperatures and drive current conditions conducting to huge acceleration factors (above 300–400) to reach 90% of UCL. A new and original approach consists in statistic computations to extrapolate lifetime distribution and failure rates in operating conditions from physical parameters of experimental degradation laws. Cumulative failure rates and lifetime distributions are computed mixing statistic calculations (Monte Carlo approach) and equations of physical drift mechanisms versus time fitted from experimental measurements. This methodology has been applied on a batch of 24 DFB Laser diodes emitting at 1.55  $\mu\text{m}$  mounted P-up on an alumina substrate by means of a AuSn solder. In this study, only bias current drift is monitored for ageing conditions ( $T_c = 80^\circ\text{C} - P_{opt} = 10\text{ mW}$ ) and can be fitted by Eq. (5). Fig. 11 plots experimental variations of bias current versus ageing time of some DFB Laser diodes.

$$\frac{\Delta I_{op}}{I_{op}} = at^m \exp\left[-\frac{E_a}{k} \left(\frac{1}{T_{ageing}} - \frac{1}{T_{op}}\right)\right] \quad (5)$$

where  $t$ : time,  $E_a$ : activation energy,  $T_{ageing}$ : ageing temperature,  $T_{op}$ : operating (use) temperature.

Parameters ( $a, m$ ) are fitted from these curves to reach the main parameter represented by time to failure that can be extracted using the final statistic distribution based on a Monte Carlo method. The first phase consists in extrapolating the relation between ( $a, m$ ) parameters. The possible issue is to define a specific function, generally called dispersion function ( $F_{a,m}$ ), giving the distribution of ( $a, m$ ) parameters. The resolution of  $F_{a,m}$  not provide a single solution. The determination of the correlation law between  $a$  and  $m$  allows us to obtain the dispersion function by successive determination of marginal laws associated to both an arbitrary 'main' declared coordinate and the difference of the second coordinate from the correlation law. If this last law is well adapted, this difference could be considered as a second coordinate noise, independent of the first coordinate.

A new statistical homogeneous distribution of ( $a, m$ ) couples could be reconstituted by the random draw of the 'main' coordinate, followed by the random draw of the second coordinate standard deviation. The 'main' coordinate marginal distribution function is defined by the following log-normal law:

$$G(m_x, s_x) = \frac{1}{2} \left[ 1 + \operatorname{erf}\left(\frac{\ln x - m_x}{\sqrt{2}s_x}\right) \right] \quad (6)$$

with  $m_x$ : mean value of  $\ln(x)$  and  $s_x$ : standard deviation of  $\ln(x)$ .

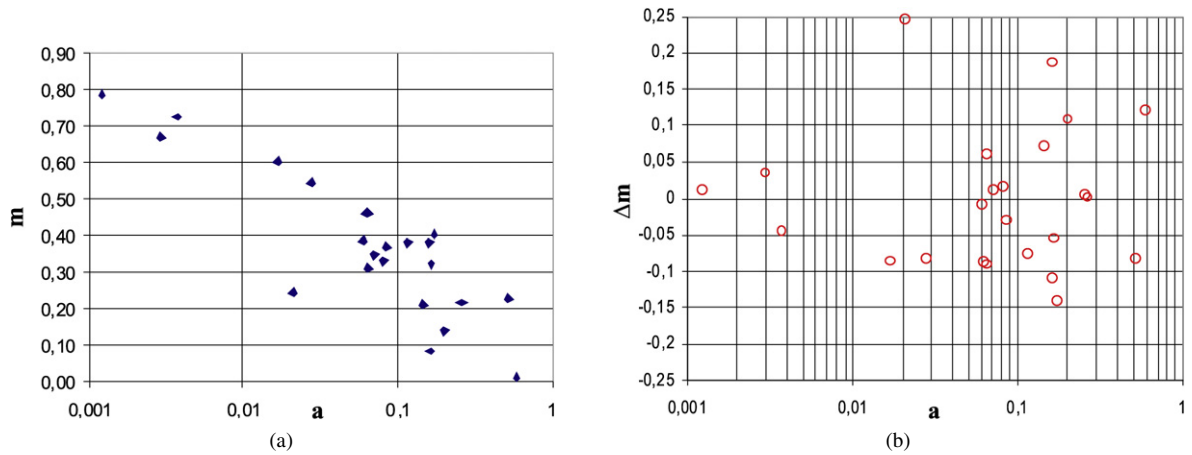


Fig. 12. (a) Experimental  $(a, m)$  couples distribution; (b) Residual error  $\Delta m$  between experimental  $(a, m)$  couples distribution and  $m = f(a)$  correlation law.

Fig. 12. (a) Distribution des couples  $(a, m)$  expérimentaux ; (b) Erreur résiduelle  $\Delta m$  entre la distribution des couples  $(a, m)$  expérimentaux et la loi de corrélation  $m = f(a)$ .

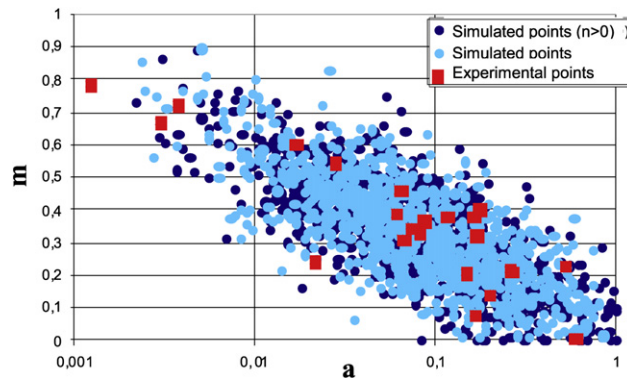


Fig. 13. Simulated and experimental distribution of  $(a, m)$  couples.

Fig. 13. Distribution simulée et expérimentale des couples  $(a, m)$ .

In this study,  $m$  is ranging from 0.1 to 0.8 and  $E_a$  is equal to 0.6 eV, corresponding to an intrinsic failure mechanism related to misfits located between active and blocking layers [27]. Fig. 12(a) shows  $m = f(a)$  distribution coming from the  $(a, m)$  couple extraction of experimental bias current versus ageing time. The choice of the correlation law is empirical: a correlation  $m_0 = A \ln(a) + B$ , with  $m$  as second coordinate is the best adapted in these experiments. The correlation law between  $a$  and  $m$  is given by:

$$m = A \ln(a) + B \quad (7)$$

with  $A = -0.10805$ ,  $B = 0.075174$  and  $R^2 = 0.88$ .

Fig. 12(b) plots the residual error  $\Delta m$  calculated between experimental points and correlation law using the RMS method. This last result assumes that the noise of the second coordinate is independent of the first chosen coordinate and confirms the good solution of the correlation law. A second step consists in an evaluation of the distribution of the parameter ( $a$ ) by a similar log-normal law as previously given in Eq. (6).

Fig. 13 displays the superposition of experimental and calculated points resulting from the statistical Monte Carlo method (4000 samples). Distribution of times to failure  $t_{eol}$  is calculated according the following equation:

$$t_{eol} = \left( \frac{k}{a} \right)^{1/m} \quad (8)$$

with  $k$  the chosen failure criterion.

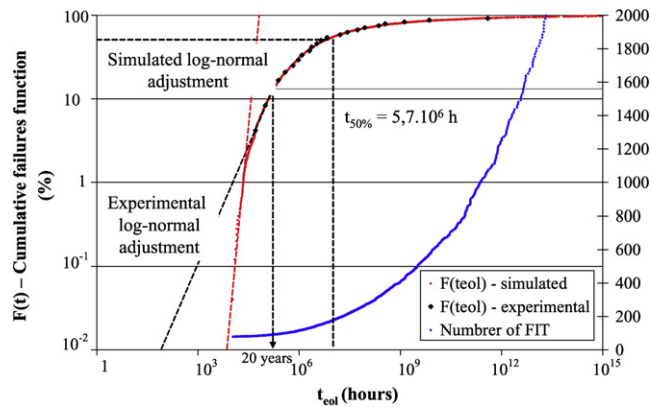


Fig. 14. Cumulative failure function  $F(t_{eol})$  and failure rate calculated for operating conditions (25 °C–10 mW).

Fig. 14. Fonction de défaillances cumulées  $F(t_{eol})$  et taux de défaillance calculé en conditions opérationnelles (25 °C–10 mW).

In this study,  $k$  corresponds to a 20% decrease of the initial bias current. Using the complete couples distribution of  $(a, m)$  plots in Fig. 13, it is possible to evaluate the time to failure  $t_{eol}$  distribution using Eq. (8). The cumulative distribution of lifetime is plotted in Fig. 14, allowing us to perform an extrapolation law adjustment for lower  $t_{eol}$  until 10% of the total lifetime distribution.

Considering the Henry diagram representation, a log-normal adjustment represented by a linear curve, corresponding to the best fitting of the  $F(t_{eol})$  law and performed both for experimental and simulated distribution, shows an important difference of extrapolation for first times to failure between the two contributions. The first times to failure extrapolation until 10% of cumulative is realized with only two points among 24 ( $\approx 10\%$ ) for experimental  $F(t_{eol})$  and with 250 points/2500 ( $= 10\%$ ) for simulated one.

The strong interest of this methodology is to largely increase the number of couples  $(a, m)$  using a Monte Carlo method, allowing us to ensure the choice of the log-normal law, used to extrapolate first times to failure with the best accuracy as possible. But it is necessary to have a good correlation between experimental and simulated  $F(t_{eol})$  curves and related to a very low residual error  $\Delta m$ . The failure rate can be determined using a lifetime distribution calculated for operating conditions (25 °C–10 mW) and is close to 100 FITs over 20 years for this technology.

## 5. Conclusion

Nanotechnology is now emerging, where device sizes will be in the range of several nanometers, leading to a high degree of failure, due to intrinsic manufacturing defects, transient faults and faults due to ageing because of molecular and other new processing for producing nanodevices. The significant gap with failure rates actually required will not be tolerated for a long time. The notion of yield of manufacturing processes is also one of the main challenges of the semiconductor industry, to avoid negative impacts on time-to-market and to increase profitability [20]. Built-in reliability of nanodevices must start taking into account aspects of criticality with respect to the constraints, from the moment of the first technological choices. It also implies the identification and characterization of failure mechanisms, considering in particular mechanical, thermal, chemical aspects related to the diversity of materials used with an additional difficulty due to the ‘ultimate’ character of dimensional parameters. The use of advanced FEM physical simulations makes possible the analysis of such devices regarding their dimensional complexity and their technological variety. They allow us to analyze local effects and to propose generic reliability tests, common to different configurations or active constraints. The effects of technological dispersion must be also analyzed and minimized. It will be also necessary to consider that most physical phenomena are discrete (for instance, density of states in quantum dot structures) and thus that the global representation in the form of continuous ‘macroscopic’ degradation law (i.e. related to parameters drift) will constitute a huge challenge to be solved. The multidisciplinary side of such an approach is absolutely essential including both questions related to physics and physico-chemistry of materials, electrical phenomena, thermal phenomena, mathematical models of data processing . . .

The objective of this paper focused on new, original, complementary solutions for reliability assessment, coming from studies of the IMS Laboratory in close collaboration with industrial and academic partners. These new

approaches are based on the combination of physical laws of failure, behavioral simulations and statistical methods taking into account the low number of samples and inevitable parametric dispersions to extrapolate failure rates and lifetime in operating conditions. Some examples have been presented and discussed in particular on micro-assembled technologies and photonic components for high-rate optical links. The main goal was to analyze their potentiality and applicability field in view of nanodevices intrinsic reliability assessment in operating conditions.

The first case deals with some results in order to derive reliability behavior of highly integrated microassemblies (BGA, Flip-Chip, CSP . . .) submitted to a thermal cycle mission profile. We have shown that a closer look is required if this extrapolation concerns a low percentiles of failures (i.e. distribution tail of early failures). Due to numerous non-linear effects involved in degradation kinetics, the reliability characteristic functions may be extremely affected by technological (and environmental) parameter dispersion. We have considered the dispersion of the ball height of BGA and CSP packages, based on process data, to obtain the total shear strain distribution by FEM simulations. These values, introduced in the analytical expression of the main degradation law (coarsening of lead phases), were used to generate a virtual distribution of numbers of cycles to failure for the two configurations, scaled to fit the experimental results. A whole virtual distribution under other conditions has been extrapolated by using the corresponding acceleration factor deduced from parameter actualization in the generic degradation law.

The addition of distributed technology parameters in new reliability models is currently a step that must be required and developed. In complementarity with other research teams considering intrinsic fluctuations ('bottom-up' approach) in relation with the decrease of dimensions (nanoelectronics), it will be necessary to also focus on techniques to control manufacturing processes allowing us to include dispersions of critical parameters. These studies will address new devices such as photonic components, III–V transistors, CNTFET, etc., micro-assembling technologies and micro/nanosystems. In the short term, the next important step, in such methodology, would now be to take into account the mission profile distributions to achieve a realistic modeling of calculated failure distributions, but also analyze the impact of components malfunctioning on electrical and/or optical performances using system simulations [28].

The second case is dedicated to optoelectronic semiconductor components (1.55  $\mu\text{m}$  DFB Laser diodes) for high-rate optical telecommunication applications, where selection tests and life testing are specifically used for reliability evaluation according to standards requirements. Unfortunately, in the case of a low number of components, there is a growing complexity to calculate average lifetime and failure rates (FITs) using ageing tests in particular due to extremely low failure rates. For actual laser diode technologies, time to failure tends to be  $10^5$  hours, aged under typical conditions. These ageing tests must be performed on more than 100 components aged during at least 10 000 hours mixing different temperatures and drive current conditions conducting to acceleration factors above 300–400. These conditions are high-cost, time consuming and cannot give a complete distribution of time to failure.

We have presented an original approach consisting in implementation of statistic computations (Monte Carlo) to extrapolate lifetimes distribution and failure rates in operating conditions from physical parameters of experimental degradation laws (i.e.  $a t^m$  power law). Cumulative failure rates and lifetime distributions are computed using statistic calculations and equations of drift mechanisms versus time fitted from experimental measurements. One of the main advantages of this methodology is to largely increase the number of couples  $(a, m)$  using a Monte Carlo method allows us to ensure the choice of the log-normal law, used to extrapolate first time to failure.

These statistic computations have been developed based on bias current drifts of 1550 nm DFB Laser diodes extrapolated using analytical power law. Nevertheless, degradation of semiconductor lasers is usually evaluated by changes in operating current, but also threshold current, emission optical power, output efficiency, central wavelength, linewidth, etc., but the origin of the failure is frequently unknown. In this context, on-going activities for reliability demonstration of nanotechnologies must necessary take into account further physical approach as proposed for example by D.T. Cassidy introducing multi-component model (MCM). The MCM describes the aging behavior in terms of multiple degradation modes with different rates of reaction. This kind of model implements depletion of raw material for growth of non-radiative recombination defects, and thus shows saturation in the change of threshold current with time describing annealing effects in the presence of such degradation [29,30].

## References

- [1] H. Iwai, Future of nano-CMOS technology and its production, in: International Symposium on the Physical & Failure Analysis of Integrated Circuits – IPFA Keynote Address, 2006, p. 1.
- [2] A.R. Brown, A. Asenov, J.R. Wailing, Intrinsic fluctuations in sub 10-nm double-gate MOSFETs introduced by discreteness of charge and matter, IEEE Nanotech. (2002) 195.

- [3] W.F. Clark, T.G. Ference, S.W. Mittl, J.S. Burnham, E.D. Adams, Improved hot-electron reliability in high-performance, multi-level CMOS using deuterated barrier-nitride processing, *IEEE El. Dev. Lett.* 20 (1999) 501.
- [4] C.H. Ming Ta, G. Zhang, Z. Gan, Dynamic study of the physical processes in the intrinsic line electromigration of deep-submicron copper and aluminium interconnects, *IEEE Dev. Mat. Reliab.* 4 (2004) 450.
- [5] R.C.J. Wang, C.C. Lee, L.D. Chen, K. Wu, K.S. Chang-Liao, A study of Cu/Low-k stress-induced voiding at via bottom and its microstructure effect, *Microelectron. Reliab.* 46 (2006) 1673.
- [6] J.S. Chen, M.D. Ker, Impact of MOSFET gate-oxide reliability in CMOS operational amplifiers in a 130 nm low-voltage CMOS process, in: *International Reliability Physics Symposium-IRPS*, 2006, p. 423.
- [7] R. Difrenza, P. Llinares, G. Ghibauda, A new model for the current factor mismatch in the MOS transistor, *Solid State Electron.* 47 (2003) 1167.
- [8] S. Lucas, Realization and SEM observation of polysilicon and aluminium cantilever using surface micromachining technology, in: *MSE 99*, Arlington, VA, USA, 1999.
- [9] Y. Zorian, Nanoscale design & test challenges, *IEEE Computer* 38 (2005) 36.
- [10] C. Constantinescu, Trends and challenges in VLSI circuit reliability, *IEEE Micro* 23 (2003) 14.
- [11] R. Baumann, Soft errors in advanced computer systems, *IEEE Design & Test of Computers* 22 (2005) 258.
- [12] S.P. Kumar, Micro-sensors networks, electronics and biology, in: *International Symposium on Advanced Electronics for Future Generations*, Tokyo, Japan, 2005, p. 23.
- [13] D. Ji, X. Gao, X.Y. Kong, J.M. Li, Atomistic failure mechanism of single wall carbon with small diameters, *Chin. Phys. Lett.* 24 (2007) 165.
- [14] J. Jimenez, Laser diode reliability: Crystal defects and degradation modes, *C. R. Physique* 4 (2003) 663.
- [15] M. Bettiat, C. Starck, M. Pommies, N. Broqua, G. Gelly, M. Avella, J. Jimenez, I. Asaad, B. Orsal, J.M. Peransin, Gradual degradation in 980 nm InGaAs/AlGaAs pump laser, *Mat. Sci. Eng. B* 91–92 (2002) 486.
- [16] B. Cluzel, L. Lalouat, P. Velha, E. Picard, D. Peyrade, J.-C. Rodier, T. Charvolin, P. Lalanne, E. Hadji, F. de Fornel, Nano-manipulation of confined electromagnetic fields with a near-field probe, *C. R. Physique* 9 (1) (2008) 24–30.
- [17] P. Senn, Objets communicants et nanotechnologies, *Revue de l'Electricité et de l'Electronique (REE): D-“Nanosciences et Radioélectricité”* (2007).
- [18] S.M. Bachilo, L. Balzano, J.E. Herrera, F. Pompeo, D. Resasco, Narrow ( $n, m$ )-distribution of single-walled carbon nanotubes grown using a solid supported catalyst, *J. Am. Chem. Soc.* 125 (2003) 11186.
- [19] G.H. Jeong, A. Yamakazi, S. Suzuki, H. Yoshimura, Y. Kobayashi, Y. Homma, Cobalt-filled apoferritin for suspended single-walled carbon nanotube growth with narrow diameter distribution, *J. Am. Chem. Soc.* 127 (2005) 8328.
- [20] D.T. Franco, J.F. Navinier, L. Navinier, Yield and reliability issues in nanoelectronic technologies, *Ann. Télécommun.* 61 (2006) 1247.
- [21] J.Y. Deletage, F. Verdier, B. Plano, Y. Deshayes, L. Bechou, Y. Danto, Reliability estimation of BGA and CSP assemblies using degradation law model and technological parameters deviation, *Microelectron. Reliab.* 43 (2003) 1137.
- [22] J.Y. Deletage, Etude de la durée de vie d'assemblages microélectroniques par l'utilisation de simulations, de modèles de dégradation et de circuits intégrés spécifiques de test, PhD. Thesis, Université Bordeaux 1, France, 2003.
- [23] J.W. Ewans, Simulation of fatigue distributions for ball grid arrays by the Monte-Carlo method, *Microelectron. Reliab.* 40 (2000) 1147.
- [24] L. Mendizabal, L. Bechou, Y. Deshayes, F. Verdier, Y. Danto, D. Laffitte, J.L. Goudard, F. Houe, Study of influence of failure modes on lifetime distribution prediction of 1.55  $\mu\text{m}$  DFB laser diodes using weak drift of monitored parameters during ageing tests, *Microelectron. Reliab.* 44 (2004) 1337.
- [25] Y. Deshayes, L. Bechou, F. Verdier, B. Tregon, D. Laffitte, J.L. Goudard, Y. Hernandez, Y. Danto, Estimation of lifetime distributions on 1550 nm DFB laser diodes using Monte-Carlo statistic computations, in: *SPIE Photonics Europe Conference 5465*, Strasbourg, France, 2004, p. 103.
- [26] S. Huyghe, L. Bechou, N. Zerounian, Y. Deshayes, F. Aniel, A. Denolle, D. Laffitte, J.L. Goudard, Y. Danto, Electroluminescence spectroscopy for reliability investigations of 1.55  $\mu\text{m}$  bulk semiconductor optical amplifier, *Microelectron. Reliab.* 45 (2005) 1593.
- [27] O. Ueda, *Reliability and Degradation of III-V Optical Devices*, Artech House, Boston, 1996.
- [28] L. Bechou, L. Mendizabal, C. Aupetit-Berthelemot, Y. Deshayes, J.M. Dumas, J.L. Goudard, Y. Danto, Performance and reliability predictions of 1550 nm WDM optical transmission links using a system simulator, in: *SPIE Photonics Europe Conference 6193*, Strasbourg, France, 2006, pp. 13–1.
- [29] S.K.K. Lam, R.E. Mallard, D.T. Cassidy, Analytical model for saturable aging in semiconductor lasers, *J. Appl. Phys.* 94 (2003) 1803.
- [30] S.K.K. Lam, R.E. Mallard, D.T. Cassidy, An extended multi-component model for the change of threshold current of semiconductor lasers as a function of time under the influence of defect annealing, *J. Appl. Phys.* 95 (2004) 2264.